10.37021/ijper.v8i1.03

RESEARCH ARTICLE

Design and Computational Evaluation (Docking) of quinazoline–piperazine carboxamide derivatives as Potential Tyrosine Kinase Inhibitors

Shikha Sharma*, Abhishek Kashyap, Pallavi Manish Lavhale, Pushkar Kumar Ray

ABSTRACT

The abnormal regulation of c-ABL tyrosine kinase linked with the BCR-ABL fusion gene remains the primary therapeutic focus in the management of Chronic Myeloid Leukemia (CML). While inhibitors such as Imatinib have shown notable clinical efficacy, the development of resistance mutations creates the need for new therapeutic candidates. In this regard, the present study reports the rational design and computational screening of a novel set of compounds, namely quinazoline–piperazine carboxamide derivatives, as prospective ATP-competitive inhibitors. These hybrid molecules were designed by merging the kinase inhibitory characteristics of the quinazoline core with the structural properties of the piperazine-carboxamide moiety. Molecular docking studies against the c-ABL kinase domain (PDB ID: 1IEP) identified high-affinity lead compounds with strong structural compatibility in the ATP-binding pocket. Interaction analysis demonstrated stable hydrogen bond formation in the hinge region along with notable stabilization of the DFG motif, indicating the anticancer potential of these derivatives. These outcomes offer a strong theoretical basis for further chemical synthesis and biological evaluation.

Keywords: Keywords.

How to cite this article: Sharma S, Kashyap A, Lavhale PM, Ray PK. Design and Computational Evaluation (Docking) of quinazoline–piperazine carboxamide derivatives as Potential Tyrosine Kinase Inhibitors. Int. J. Pharm. Edu. Res. 2026;8(1):17-26.

Source of support: Nil

Conflict of interest: None

INTRODUCTION

Chronic Myeloid Leukemia (CML) is a clonal myeloproliferative disorder marked by the presence of the Philadelphia chromosome (Ph). This cytogenetic alteration originates from a reciprocal translocation between chromosomes 9 and 22, represented as t(9;22)(q34;q11). This rearrangement leads to the fusion of the BCR (breakpoint cluster region) gene with the ABL1 (Abelson murine leukemia viral oncogene homolog 1) gene.[1-3] The ABL kinase domain exhibits a bilobed architecture, consisting of an N-terminal lobe formed by β-sheets and an α-helix (C-helix), and a C-terminal lobe predominantly made up of α-helices. The ATP-binding pocket is located between these two lobes and serves as the main site for catalytic activity. Tyrosine Kinase Inhibitors (TKIs) are designed to competitively bind to this pocket, thereby blocking ATP binding and inhibiting the phosphorylation of substrate proteins. The clinical success of Imatinib (Gleevec), the first-in-class TKI, established BCR-ABL as a "gold standard" therapeutic target in CML, converting a previously fatal disease into a manageable chronic condition. Despite the early success of TKIs, the development of drug resistance continues to be a major clinical concern. Resistance commonly arises due to point mutations within the ABL kinase domain that disrupt drug binding. Among these, the T315I "gatekeeper" mutation is the most significant, where Threonine is substituted by Isoleucine at position 315.[4] This alteration removes an essential hydrogen bond and introduces steric hindrance, making first- and second-generation TKIs such as Imatinib and Nilotinib ineffective. Although third-generation inhibitors like Ponatinib can overcome this mutation, they are linked with serious cardiovascular toxicity and vascular occlusion, thereby emphasizing the need for safer and more effective scaffolds.[5,6]

In efforts to develop potent and selective TKIs, the quinazoline scaffold has gained considerable importance. Structurally, the quinazoline ring system functions as a bioisostere of adenine, the purine base of ATP. These inhibitors act in an ATP-competitive manner and are capable of forming one to three hydrogen bonds with amino acid residues present in the hinge region of the target kinase, thereby replicating the interactions typically formed by the adenine ring of ATP. This property enables quinazoline derivatives to establish crucial hydrogen-bonding interactions within the hinge region of the ABL kinase domain, effectively mimicking the binding mode of natural nucleotides.[7,8]

The present study focuses on the rational, structure-based design of quinazoline–piperazine carboxamide

Ram Eesh Institute of Vocational and Technical Education, 3, knowledge park I, Greater Noida – 201310.

Corresponding Author: Shikha Sharma, Ram Eesh Institute of Vocational and Technical Education, 3, knowledge park I, Greater Noida – 201310., E-mail: shikhabhardwaj2728@gmail.com

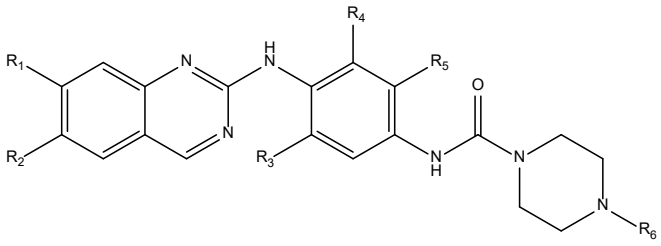

Figure 1: General structure of quinazoline–piperazine carboxamide derivatives showing different substitution positions (R_1-R_6).

derivatives. By introducing an aniline moiety at the 4-position, the aim is to improve hydrophobic interactions and van der Waals forces within the enzyme's hydrophobic regions, such as the P-loop or the selectivity pocket. This work employs computational molecular docking to examine the binding affinities and detailed residue-level interactions of the designed ligands with the crystal structure of the ABL kinase. In addition, their pharmacokinetic (ADME) properties are evaluated to confirm drug-likeness and reduce potential off-target toxicities, thereby offering a theoretical basis for the development of a new class of anti-CML agents.

Clinical Challenges & Limitations of Imatinib

- Emergence of Acquired Resistance
- Development of Point Mutations in the BCR-ABL kinase domain.
- The T315I "Gatekeeper Mutation" creates steric hindrance, preventing Imatinib from binding.
- Selectivity:
- Inhibition of non-target kinases like c-KIT and PDGFR.
- Leads to clinical side effects: Cardiotoxicity, Edema, and Gastrointestinal distress.
- Disease Progression & Relapse
- Sub-optimal binding affinity in mutated cases leads to treatment failure and cancer recurrence.

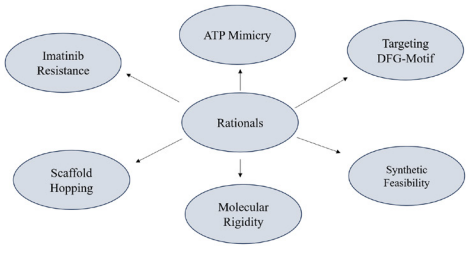

Figure 2: Conceptual framework and rationales for the development of targeted Tyrosine Kinase inhibitors.

Rational Design Strategy for Novel ABL Kinase Inhibitors

The rational molecular design of the novel quinazoline–piperazine carboxamide derivatives was based on a multifaceted pharmacophore integration strategy, combining established design features to achieve potent and selective inhibition of the BCR-ABL tyrosine kinase. Despite the availability of first- and second-generation Tyrosine Kinase Inhibitors (TKIs), the need for these new derivatives arises due to ongoing clinical issues such as multidrug resistance and systemic toxicity. Although third-generation inhibitors like Ponatinib can address critical mutations, they are frequently associated with serious cardiovascular side effects. The present design seeks to address these limitations by developing molecules that offer strong activity against resistant variants while ensuring an improved safety profile and ease of synthesis.

A key aspect of the design was the application of ATP mimicry, a well-established concept employed in several approved anticancer drugs such as Gefitinib for lung cancer and Lapatinib for breast cancer. By employing the quinazoline scaffold as an adenine bioisostere, the design facilitates effective occupation of the ATP-binding pocket. This core enables the molecule to anchor within the hydrophobic environment of the hinge region, replicating the binding architecture of second-generation inhibitors like Nilotinib, even without the formation of conventional hydrogen bonds with the Met318 residue.[9,10,11] A major goal of this rational design was to overcome Imatinib resistance, which mainly results from point mutations in the ABL kinase domain. The most prominent among these is the T315I "gatekeeper" mutation, in which a Threonine residue is replaced by a bulky and hydrophobic Isoleucine. In the case of Imatinib, this mutation leads to resistance by removing a crucial hydrogen bond and introducing significant steric hindrance at the entrance of the binding pocket, thereby preventing the drug from accessing the catalytic site.[12,13]

To address this limitation, the present study employed a scaffold hopping strategy, moving toward a hybrid framework that incorporates a flexible piperazine-1-carboxamide moiety. This flexible linker serves as a structural "tail," enabling the derivative to adjust its conformation while approaching the binding site. In contrast to the relatively rigid structure of Imatinib, which experiences steric clash with the bulky Isoleucine residue at the "gate," the designed derivatives can reorient themselves to bypass the mutated gatekeeper through an alternative spatial pathway. Once within the binding site, the molecule adopts a "distal binding strategy," positioning the quinazoline–aniline core in

hydrophobic regions that are not affected by the T315I substitution. The major contribution to binding energy is directed deeper into the pocket to target the DFG motif, particularly through interactions with the conserved residues Glu286 and Asp381. By stabilizing the enzyme in its "DFG-out" (inactive) conformation, these derivatives are capable of locking the kinase in a non-functional state. This integrated design approach ensures that the lead compounds retain inhibitory activity against both wild-type and mutant BCR-ABL kinase, providing a strong theoretical basis for the development of safer, selective, and cost-effective therapeutic agents for Chronic Myeloid Leukemia (CML).[14]

MATERIALS AND METHODS

Docking Work Performed

Hardware and software utilised in the study

For the present molecular docking studies, a 64-bit HP laptop running Windows 11 Home Single Language, powered by an Intel(R) Core™ i3-8130U processor operating at 2.21 GHz, with 8 GB of RAM and a 256 GB SSD, was used to perform the computational simulations.

Procedure

The crystal structure of the target protein, the C-ABL tyrosine kinase domain, was obtained from the RCSB Protein Data Bank (https://www.rcsb.org). The protein was carefully prepared in its Apo form using Swiss-PDB Viewer by removing the co-crystallized inhibitor (Imatinib), water molecules, and all non-standard heteroatoms, and then saved as a separate PDB file to be used as the docking receptor.[15,16,17] The ligand library, together with the prepared Apo-protein, was subsequently imported into the PyRx virtual screening platform. Through the AutoDock Vina wizard integrated within PyRx, the SDF files were processed and converted into PDBQT format, which is required for grid-based energy calculations.[18] The docking grid box was appropriately centered on the ATP-binding site (hinge region) of the ABL kinase to ensure accurate ligand–receptor interactions.[19] For post-docking analysis and detailed 3D visualization of the protein–ligand complexes, BIOVIA Discovery Studio Visualizer 2020 was employed to analyze binding orientations and evaluate the stability of the complexes.[20-22]

Binding site interactions of ligand with protein

To understand the molecular basis of binding affinity and to predict the stability of the drug–receptor complex, interaction patterns within the active site of the C-ABL tyrosine kinase were analyzed using BIOVIA Discovery Studio Visualizer 2020. The analysis focused on identifying the exact binding pocket, including the highly conserved hinge region, catalytic residues, and the regulatory DFG motif, all of which are essential for designing ATP-competitive inhibitors for Chronic

Table 1: Designed 15 molecules from scaffold (Fig: 1) and their obtained docking score by docking studies.

S.No.	*Ligand*	*Positions of R*			*Docking Score*
1	IMitinib	NA	NA	NA	-13.4
2	Ligand_1_uff_E=701.62	R1 -OH	-	R6 -OH	-10.2
3	Ligand_2_uff_E=740.67	R2 -OCH3	-	R6 -OH	-8.9
4	Ligand_3_uff_E=648.83	R1 -OH	-	R6 -OCH3	-9.6
5	Ligand_4_uff_E=695.43	R1-F	-	R6 -OH	-9.9
6	Ligand_5_uff_E=799.47	R1 -F	-	R6 -CH2CH2OH	-9.7
7	Ligand_6_uff_E=647.61	R1 -OH	-	R6 -CH2CH2OH	-9.3
8	Ligand_7_uff_E=977.78	R1 -OCH3 R2 -OCH3	-	R6 -CH2CH2OH	-8.5
9	Ligand_8_uff_E=771.97	R1 -OH	R3 -CH3	R6 -CH2CH2OH	-9.6
10	Ligand_9_uff_E=857.30	R2 -OCH3	R5 -F	R6 -CH2CH2OH	-10.1
11	Ligand_10_uff_E=710.22	R1 -OCH3	-	R6 -CH2CH2OH	-9.4
12	Ligand_11_uff_E=619.64	R1 -OH	R5 -NH2	R6 -CH2CH2OH	-9.1
13	Ligand_12_uff_E=643.27	R1 -OH	R4 -OH	R6 -CH2CH2OH	-9.3
14	Ligand_13_uff_E=757.55	R1 -OH	R5 -OH	R6 -CH2CH2OH	-9.5
15	Ligand_14_uff_E=1411.27	R1 -OH	R5 -OH	-	-10.4
16	Ligand_15_uff_E=738.06	-	R5 -OH	R6 -CH2CH2OH	-9.6

Table 2: The best six docking score derivatives from scaffold (Fig: 1).

S. No.	Ligand	Docking score
1	Ligand_1_uff_E=701.62	-10.2
2	Ligand_4_uff_E=695.43	-9.9
3	Ligand_5_uff_E=799.47	-9.7
4	Ligand_9_uff_E=857.30	-10.1
5	Ligand_13_uff_E=757.55	-9.5
6	Ligand_14_uff_E=1411.27	-10.4

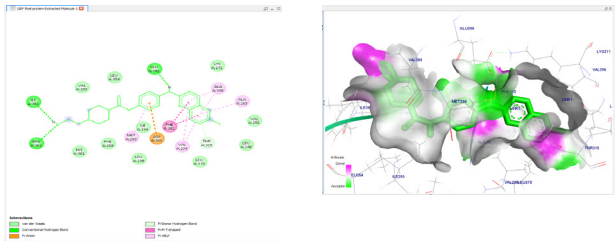

Figure 5: 3d and 2d images of binding interactions of ligand 5 with residues of 1IEP.

Table 3: Molecular interactions of top scoring ten ligands and reference ligand.

S. No.	*Ligand Code*	*No of conventional hydrogen bonds*	*H- bond forming residue*	*H-bond Distance (Å)*	*Hydrophobic residues*
1.	Original ligand	5	MET318, ASP381, THR315, GLU286, MET290	2.88 – 3.30	LEU248, THR315, PHE317, TYR253, ALA269, VAL289, VAL256, LYS271, LEU370, ILE313, MET290
2.	Ligand 1	1	GLU286	1.74	PHE382, MET290, LYS271, VAL299, ALA380, ALA269
3.	Ligand 4	1	GLU282	2.25	VAL289, LEU354, ASP381 (Pi-Anion)
4.	Ligand 5	3	ARG362, GLU286, ILE360	1.75 – 2.48	PHE382, MET290, VAL299, ASP381 (Pi-Anion)
5.	Ligand 9	2	GLU282	2.18 – 2.38	PHE382, ALA269, LEU248, ASP381 (Pi-Anion)
6.	Ligand 14	1	GLU 286	2.11	PHE382, MET290, VAL299, ASP381 (Pi-Anion)
7	Ligand 15	1	GLU 282	2.40	VAL289, LEU354, ASP381 & GLU286 (Pi-Anion)

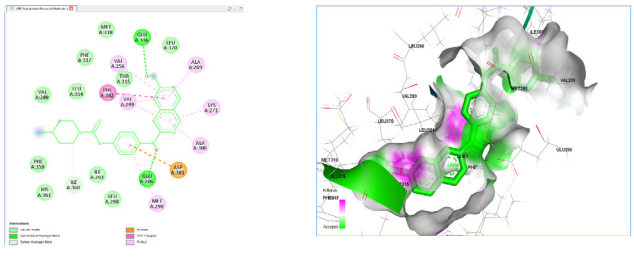

Figure 3: 3d and 2d images of binding interactions of ligand 1 with residues of 1IEP.

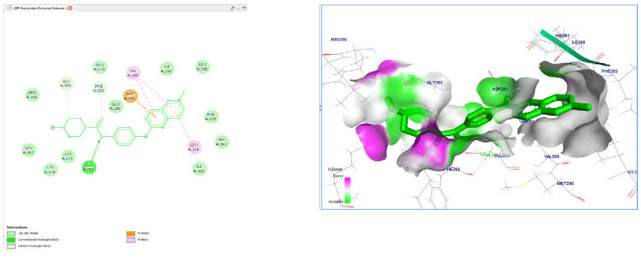

Figure 4: 3d and 2d images of binding interactions of ligand 4 with residues of 1IEP.

Myeloid Leukemia (CML).[23,6] The virtual screening platform evaluated a library of 15 rationally designed compounds (Table 1), from which the top-performing derivatives were identified based on their outstanding binding energies (Table 2).

The visualization results confirmed that the quinazoline–piperazine carboxamide derivatives effectively occupied the targeted ATP-binding domain. To further validate this, the binding orientation of the designed ligands was compared with that of the co-crystallized reference ligand, Imatinib (PDB ID: 1IEP). The results showed

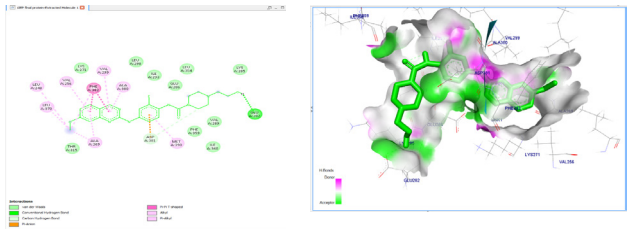

Figure 6: 3d and 2d images of binding interactions of ligand 9 with residues of 1IEP.

Table 4: ADME studies data of top six molecules of scaffold 1

Molecule	*Original ligand*	*1*	*4*	*5*	*9*	*14*	*15*
MR	154.50	112.46	110.40	120.45	128.94	113.88	122.51
TPSA	86.28	113.85 A^2	93.62	93.62	102.85	122.64	113.85
ILOGP	4.04	2.43	2.88	3.33	3.69	2.33	3.01
XLOGP3	3.52	1.57	2.03	1.83	1.89	1.24	1.38
WLOGP	3.49	1.67	2.52	2.12	2.13	1.27	1.27
MLOGP	2.15	1.41	2.30	1.94	1.85	0.87	1.06
Silicos-IT Log P	3.69	-0.21	0.09	1.46	1.52	0.36	0.56
Consensus Log P	3.38	1.37	2.08	2.14	2.18	1.21	1.45
ESOL Log S	-5.07	-3.28	-3.58	-3.47	-3.55	-3.07	-3.17
ESOL Solubility (mg/mL)	4.20e-03	1.99e-01	1.003-01	1.39e-01	1.25e-01	3.22e-01	2.73e-01
ESOL Solubility (Mol/l)	8.51e-06	5.24e-04	2.61e-04	3.39e-04	2.84e-04	8.46e-04	6.69e-04
ESOL Class	Moderately soluble	Soluble	Soluble	Soluble	Soluble	Soluble	Soluble
Ali Log S	-5.02	-3.57	-3.62	-3.42	-3.58	-3.41	-3.37
Ali Solubility (mg/mL)	4.78e-03	1.02e-04	9.09e-02	1.57e-01	1.18e-01	1.46e-01	1.73e-01
Ali Solubility (mol/l)	9.68e-06	2.68e-04	2.38e-04	3.84e-04	2.68e-04	3.86e-04	4.23e-04
Ali Class	Moderately soluble	Soluble	Soluble	Soluble	Soluble	Soluble	Soluble
Silicos-IT LogSw	-9.67	-4.47	-5.32	-6.11	-6.21	-5.18	-5.25
Silicos-IT Solubility (mg/mL)	1.05e-07	1.293-02	1.83e-03	3.22e-04	2.74e-04	2.50e-03	2.28e-03
Silicos-IT Solubility (mol/l)	2.12e-10	3.40e-05	4.79e-06	7.83e-07	6.22e-07	6.58e-06	5.57e-06
Silicos-IT class	Poorly soluble	Moderately soluble	Moderately soluble	Poorly Soluble	Poorly soluble	Moderately soluble	Moderately soluble
GI absorption	High	High	High	High	High	High	High
BBB permeant	No	No	No	No	No	No	No
Pgp substrate	Yes	Yes	Yes	Yes	Yes	Yes	No
CYP inhibition	Yes (2C19, 2C9,2D6,3A4)	Yes (1A2)	Yes (1A4)	Yes (2D6, 3A4, 3A4)	Yes (2D6, 3A4)	Yes (1A2)	No
log Kp (cm/s)	-8.81	-7.51 cm/s	-7.19 cm/s	-7.50	-7.71	-7.74	-781 cm/s
Lipinski violations	0	0	0	0	0	0	0
Ghose violations	2	0	0	0	0	0	0
Veber violations	0	0	0	0	0	0	0
Egan violations	0	0	0	0	0	0	0
Muegge violations	0	0	0	0	0	0	0
Bioavailability score	0.55	0.55	0.55	0.55	0.55	0.55	0.55
PAINS alerts	0 alert	0 alert	0 alert	0 alert	0 alert	0 alert	0 alert

Brenk alerts	0 alert	0 alert	0 alert	0 alert	0 alert	1 alert (catechol)	1 alert (catechol)
Leadlikeness violations	3	1 violation (MW>350)	1	1	2 (MW>350, Rotors>7)	1 (MW>350)	1 (MW>350)
Synthetic accessibility	3.78	3.02	3.01	3.05	3.32	2.89	3.17

that the ligands formed key high-affinity conventional hydrogen bonds with important residues in the hinge region, particularly Met318, reflecting a typical kinase–inhibitor interaction pattern (Table 3). Specifically, the binding interactions and precise spatial orientations inside the pocket were evaluated for the lead molecules, including Ligand 1 (Figure 3), Ligand 4 (Figure 4), Ligand 5 (Figure 5), Ligand 9 (Figure 6), and Ligand 14 (Figure 7). Additionally, significant interactions were observed within the DFG (Asp-Phe-Gly) motif, especially with residues Glu286 and Asp381.[24,25,26] These hydrogen-bonding interactions play a crucial role in stabilizing the inactive conformation of the kinase, thereby preventing the conformational chanmges required for ATP binding and downstream signaling. Alongside these electrostatic interactions, notable hydrophobic interactions, including π–π stacking and π–alkyl interactions, were identified with nearby hydrophobic residues such as PHE317, LEU248, and TYR253, which help in anchoring the ligand within the binding pocket and enhancing its residence time. The interaction mapping and validation confirm that the quinazoline–piperazine carboxamide derivatives bind specifically to the recognized therapeutic sites of the C-ABL kinase (Fig 1).

Protein Preparation

The X-ray crystallographic structure of the C-ABL tyrosine kinase domain complexed with its native ligand (Imatinib), identified by PDB ID: 1IEP, was used as the primary biological target for this study.[27] The high-resolution 3D structural data were obtained from the RCSB Protein Data Bank (https://www.rcsb.org), ensuring all-atom validation in accordance with established crystallographic standards.

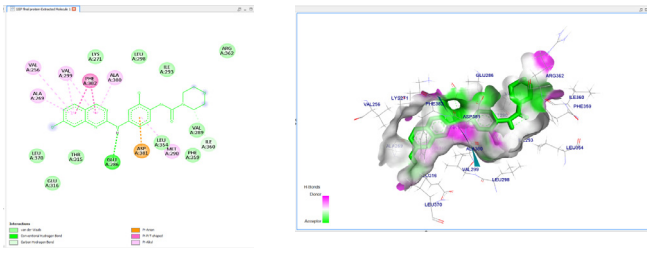

Figure 7: 3d and 2d images of binding interactions of ligand 14 with residues of 1IEP.

To achieve accurate docking simulations, the MOLPROBITY service was applied for preparation and refinement of the protein in its Apo form. The PDB file (1IEP) was uploaded to the MOLPROBITY server, where hydrogen atoms were systematically added to satisfy valency requirements. Important refinement steps included the reorientation ("flipping") of residues such as Asparagine (Asn), Glutamine (Gln), and Histidine (His) using the Make Flipkin kinemages tool.[28,29] This process helps to optimize hydrogen-bonding networks and correct orientation issues in amide and imidazole groups that may occur during crystallization. The molecular geometry and all-atom contacts were then carefully evaluated to confirm the structural integrity of the protein. After refinement, the optimized protein structure was downloaded. The Swiss-PDB Viewer (DeepView) was subsequently used to generate the Apo-receptor by removing the co-crystallized ligand and water molecules, preparing the kinase domain for docking with the designed quinazoline–piperazine carboxamide derivatives along with the reference compound.

Ligand Preparation

The molecular docking study employed the original co-crystallized inhibitor, Imatinib, which was isolated from the protein–ligand complex (PDB ID: 1IEP) and saved as a separate structural file using Swiss-PDB Viewer (DeepView). This file was used as a standard docking reference to validate the accuracy of the virtual screening protocol. For this investigation, a library of novel quinazoline–piperazine carboxamide derivatives was rationally designed based on the known pharmacophoric features of clinically approved tyrosine kinase inhibitors. The design strategy emphasized the incorporation of key bioisosteric modifications to improve binding affinity within the ABL kinase domain while preserving suitable physicochemical properties. A total of 15 carefully designed derivatives were generated from the lead scaffold, forming a diverse chemical set for screening. All 2D molecular structures were prepared using the ACD/ChemSketch software, following the American Chemical Society (ACS) guidelines for standard chemical representation. The structural files

were then processed using the OpenBabel GUI software for format conversion and optimization.[30] To ensure accurate docking results, the ligand library was imported into the PyRx virtual screening tool, where the Open Babel wizard was applied for energy minimization, allowing each conformer to reach a stable local minimum. After optimization, the ligand structures were converted from SDF format to PDBQT format, incorporating the necessary partial charges and atom types required for the AutoDock Vina scoring function. This systematic preparation ensured that the calculated binding affinities (ΔG values) represented the most energetically favorable orientations within the BCR-ABL active site.

Docking validation

To validate the docking protocol and ensure the reliability of the binding poses, a self-docking (redocking) study was performed. The co-crystallized ligand, Imatinib, was removed from the active site of c-ABL tyrosine kinase (PDB ID: 1IEP). The protein in its apo form was prepared, and the extracted ligand was redocked into the same binding site using identical grid coordinates and docking parameters as applied for the designed compound series. The redocked pose exhibited a strong structural overlap with the original co-crystallized conformation, confirming the reliability and accuracy of the docking protocol. The optimized docking settings were subsequently used for the virtual screening of all designed quinazoline–piperazine derivatives.

Docking Execution of Prepared Protein and Ligand Library

The molecular docking simulations were carried out using the AutoDock Vina wizard integrated within the PyRx 0.8 virtual screening suite. After refinement of the protein structure using the MOLPROBITY server, the optimized Apo-protein was employed for both validation and detailed docking of the newly designed quinazoline–piperazine carboxamide derivatives. The ligand preparation involved converting the SMILES representations of all 15 designed compounds into a single SDF library using Open Babel. Within the PyRx platform, these ligands were subjected to energy minimization to obtain their most stable conformations, followed by conversion into the AutoDock PDBQT format, incorporating required atomic partial charges and solvation parameters.[31,32]

For grid-based energy evaluation, a grid box with dimensions of 25 × 25 × 25 Å along the x, y, and z axes was defined. The grid spacing was maintained at the standard value of 0.375 Å to ensure precise sampling of the binding region. The center of the grid was carefully aligned with the ATP-binding pocket (hinge region) of the ABL kinase. For the 1IEP system, the grid center coordinates were approximately set to X = −15, Y = −52, and Z = −16, based on the validated binding position of Imatinib. Docking simulations were performed with an exhaustiveness value of 15 to allow thorough exploration of ligand conformations. Finally, all generated protein–ligand complexes along with their binding affinities (kcal/mol) were examined and visualized using BIOVIA Discovery Studio Visualizer 2020 to assess molecular interactions and structural complementarity.[33]

ADME Studies and Pharmacokinetic Profiling

To assess the clinical potential and drug-likeness of the designed quinazoline–piperazine carboxamide derivatives, detailed ADME (Absorption, Distribution, Metabolism, and Excretion) studies were performed. These evaluations are crucial for predicting whether a lead compound possesses the required pharmacokinetic characteristics for effective performance in biological systems. The SwissADME web-based platform (http://www.swissadme.ch/), developed by the Molecular Modeling Group at the Swiss Institute of Bioinformatics (SIB), was used for these predictions.

The assessment included several key parameters

- Lipophilicity and Solubility: Various descriptors such as iLOGP, XLOGP3, WLOGP, MLOGP, and SILICOS-IT were analyzed to evaluate membrane permeability. Aqueous solubility was further examined using Log S models (ESOL, Ali, and SILICOS-IT).
- Pharmacokinetics: Predictions included gastrointestinal (GI) absorption, blood–brain barrier (BBB) permeability, and identification of compounds as substrates of P-glycoprotein (P-gp).
- Metabolic Profile: Particular attention was given to the inhibition potential of major cytochrome P450 enzymes, including CYP1A2, CYP2C9, CYP2C19, CYP2D6, and CYP3A4, to estimate possible drug–drug interactions.
- Drug-likeness and Medicinal Chemistry: Compliance with standard rules such as Lipinski's Rule of Five, Ghose, Veber, Egan, and Muegge criteria was evaluated. Additionally, the compounds were screened for PAINS (Pan-Assay Interference Compounds) and Brenk alerts to detect undesirable structural features, along with analysis of synthetic accessibility and bioavailability scores.

The results were obtained by submitting the SMILES (Simplified Molecular Input Line Entry System) strings of each designed derivative to the SwissADME server.

RESULTS

Performed Docking Studies

Target site identification

The molecular docking studies were directed toward the ATP-binding site of the c-ABL tyrosine kinase, a well-established therapeutic target for Chronic Myeloid Leukemia (CML). Within the binding region of the reference ligand Imatinib (PDB ID: 1IEP), key residues such as Met318, Thr315, and Glu286 were recognized as crucial for ligand stabilization. The hinge region, especially the Met318 residue, serves as the main interaction site for ATP-competitive inhibitors. In addition, residues like Asp381 and Phe382 represent the conserved DFG (Asp-Phe-Gly) motif, which plays a vital role in maintaining the inactive conformation of the kinase. To achieve complete coverage of the active site, docking was performed using an expanded grid box of 25 Å in the XYZ dimensions, centered at coordinates corresponding to the crystallized position of Imatinib. The identification of these residues within the 1IEP binding pocket confirms the presence of the catalytic domain responsible for BCR-ABL inhibition.

Validation Studies

To ensure the reliability of the computational protocol, the Vina wizard in the PyRx program was used to perform self-docking (redocking) of the native ligand, Imatinib, into the prepared apo form of the c-ABL kinase (PDB ID: 1IEP). The validation process showed that the predicted optimal docking pose of Imatinib was perfectly superimposed with its original co-crystallized orientation within the protein binding pocket. This high level of conformational similarity confirms the accuracy of the docking parameters and the scoring function employed in this study. The validation studies indicated that the binding energy for the redocked Imatinib was -13.4 kcal/mol, which serves as a reference value for assessing the newly designed quinazoline–piperazine carboxamide derivatives. The successful redocking validation ensures that the subsequent docking results for the 15 designed derivatives represent reliable binding affinities.

Swiss ADME Studies Results

By using the online SwissADME web server tool, the best six compounds with the highest docking scores compounds 1, 4, 5, 9, 14, and 15 were subjected to ADME analysis, including absorption, distribution, metabolism, and excretion (Table 4). All six compounds showed good gastrointestinal (GI) absorption, and none of them violated the standard drug-likeness parameters. They also satisfied multiple drug-likeness filters, including Lipinski's rule of five, Ghosh rule, Veber rule, Egan rule, and Muegge rule, with a bioavailability score of 0.55. Each of the selected compounds also demonstrated good synthetic accessibility. Additional physicochemical parameters such as LogP, molar refractivity, TPSA value, XLOGP3, WLOGP, and MLOGP were also calculated, as presented in Table 4. The results are presented in Table 4. It was observed that Ligand 15 showed a "No" inhibition profile against all major CYP isoforms in the SwissADME analysis, indicating that within this series, Ligand 15 may represent a safer metabolic profile by lowering the risk of drug–drug interactions.

DISCUSSION

The molecular docking analysis of the designed quinazoline–piperazine carboxamide derivatives against c-ABL kinase (PDB ID: 1IEP) indicates a deliberate shift from conventional hinge-binding inhibition. The main objective of this work was to investigate a hinge-independent binding approach by emphasizing stabilization of the regulatory DFG motif (Asp381, Phe382, and Glu286). In contrast, the reference inhibitor Imatinib shows strong thermodynamic stability of -13.4 kcal/mol, primarily through hydrogen bonding interactions with the hinge residue Met318. The designed compounds, however, display a distinct binding behavior. The docking scores of the ligands, ranging from -8.5 to -10.4 kcal/mol, suggest that although the overall binding affinity is comparatively lower, the orientation of these molecules within the active site is more directed toward the deeper allosteric region. Structural analysis from 2D interaction profiles indicates that the proposed mechanism relies on stabilizing the kinase in its inactive "DFG-out" conformation. Several lead compounds consistently form Pi-anion and hydrogen bond interactions with Asp381 and Glu286. These specific contacts with the DFG motif are proposed to restrict the conformational flexibility of the enzyme, thereby inhibiting its transition to the active state. By avoiding reliance on the Met318 hinge region, these derivatives may offer an advantage in overcoming resistance associated with gatekeeper mutations such as T315I, which commonly reduce the effectiveness of hinge-dependent inhibitors. Although direct DFG-targeting strategies have been explored previously with varying success, the present scaffold attempts to improve this approach by optimizing both structural rigidity and synthetic accessibility. In addition, the study also considers the important aspect of metabolic stability, which is a key limitation in the clinical development of tyrosine kinase inhibitors. Inhibition of Cytochrome P450 enzymes often leads to undesirable drug–drug

interactions. In this context, SwissADME screening was used as a filtering step for identifying metabolically safer candidates. Among the studied compounds, Ligand 15 was particularly notable, as it showed no inhibitory activity against major CYP isoforms (CYP1A2, CYP2C9, CYP2C19, CYP2D6, and CYP3A4), despite having moderate binding affinity. This indicates that the quinazoline–piperazine framework can potentially be optimized to achieve effective DFG-motif interaction while maintaining improved metabolic safety compared to earlier DFG-targeted inhibitors. In conclusion, although computational docking results remain predictive and require experimental validation through in vitro studies, the findings provide a coherent theoretical basis. By combining scaffold optimization with conformational locking strategies, this study suggests a possible route for designing tyrosine kinase inhibitors with reduced susceptibility to hinge-region resistance. The selection of candidates such as Ligand 15, which demonstrate a balance between DFG-site binding and minimal CYP inhibition, represents an effort to address long-standing safety challenges in this class of inhibitors.

ACKNOWLEDGMENTS

Here we would like to thanks PyRx sourceforge, Swiss Institute of Bioinformatics (SwissADME online server tool) and pkCSM online webserver tool providers for using there tools. I also express my sincere thanks to Dr. Abhishek Kashyap for his constant guidance and support in designing the molecules and completing this study.

REFERENCES

1. Lahmouad M, Rachid Z, Bellemrrabet R, et al. Mechanisms and signaling pathways of tyrosine kinase inhibitor resistance in chronic myeloid leukemia: A comprehensive review. Leuk Res Rep. 2025;24:100533.
2. Sampaio MM, Santos MLC, Marques HS, et al. Chronic myeloid leukemia-from the Philadelphia chromosome to specific target drugs: A literature review. World J Clin Oncol. 2021;12(2):69-94.
3. Lahmouad M, Rachid Z, Bellemrrabet R, et al. Mechanisms and signaling pathways of tyrosine kinase inhibitor resistance in chronic myeloid leukemia: A comprehensive review. Leuk Res Rep. 2025;24:100533.
4. Amarante-Mendes GP, Rana A, Datoguia TS, Hamerschlak N, Brumatti G. BCR-ABL1 Tyrosine Kinase Complex Signaling Transduction: Challenges to Overcome Resistance in Chronic Myeloid Leukemia. Pharmaceutics. 2022;14(1):215.
5. Lahmouad M, Rachid Z, Bellemrrabet R, et al. Mechanisms and signaling pathways of tyrosine kinase inhibitor resistance in chronic myeloid leukemia: A comprehensive review. Leuk Res Rep. 2025;24:100533.
6. Panjarian S, Iacob RE, Chen S, Engen JR, Smithgall TE. Structure and dynamic regulation of Abl kinases. J Biol Chem. 2013;288(8):5443-5450.
7. Zhang J, Yang PL, Gray NS. Targeting cancer with small molecule kinase inhibitors. Nat Rev Cancer. 2009;9(1):28-39.
8. Abdel-Mohsen HT, Anwar MM, Ahmed NS, Abd El-Karim SS, Abdelwahed SH. Recent Advances in Structural Optimization of Quinazoline-Based Protein Kinase Inhibitors for Cancer Therapy (2021-Present). Molecules. 2024;29(4):875.
9. Halder P, Rai A, Talukdar V, Das P, Lakkaniga NR. Pyrazolopyridine-based kinase inhibitors for anti-cancer targeted therapy. RSC Med Chem. 2024;15(5):1452-1470.
10. Zhang J, Yang PL, Gray NS. Targeting cancer with small molecule kinase inhibitors. Nat Rev Cancer. 2009;9(1):28-39.
11. Șandor A, Ionuț I, Marc G, Oniga I, Eniu D, Oniga O. Structure-Activity Relationship Studies Based on Quinazoline Derivatives as EGFR Kinase Inhibitors (2017-Present). Pharmaceuticals (Basel). 2023;16(4):534.
12. Cohen P, Cross D, Jänne PA. Kinase drug discovery 20 years after imatinib: progress and future directions. Nat Rev Drug Discov. 2021;20(7):551-569.
13. Soverini S, Iacobucci I, Baccarani M, Martinelli G. Targeted therapy and the T315I mutation in Philadelphia-positive leukemias. Haematologica. 2007;92(4):437-439.
14. Tuzikiewicz A, Wawrzyniak W, Kutner A, Żołek T. Advances in Targeting BCR-ABLT315I Mutation with Imatinib Derivatives and Hybrid Anti-Leukemic Molecules. Molecules. 2026;31(2):341.
15. Swain C. Open Babel Documentation. 2014.
16. O'Boyle NM, Banck M, James CA, et al. Open Babel: An open chemical toolbox. J Cheminform. 2011;3:33.
17. O'Boyle NM, Banck M, James CA, Morley C, Vandermeersch T, Hutchison GR. Open Babel. J Cheminform. 2011;3:1–14.
18. Trott O, Olson AJ. AutoDock Vina: Improving the speed and accuracy of docking with a new scoring function, efficient optimization, and multithreading. J Comput Chem. 2010;31:455-461.
19. Trott O, Olson AJ. AutoDock Vina: Improving the speed and accuracy of docking with a new scoring function, efficient optimization, and multithreading. J Comput Chem. 2010;31:455-461.
20. BIOVIA Discovery Studio [Internet]. Dassault Systèmes; c2020. Available from: https://www.3ds.com/products/biovia/discovery-studio
21. Berman HM, Westbrook J, Feng Z, Gilliland G, Bhat TN, Weissig H, Shindyalov IN, Bourne PE. The Protein Data Bank. Nucleic Acids Res. 2000;28:235–242.
22. Williams CJ, Headd JJ, Moriarty NW, et al. MolProbity: More and better reference data for improved all-atom structure validation. Protein Sci. 2018;27(1):293-315.
23. Umezawa K, Kii I. Druggable Transient Pockets in Protein Kinases. Molecules. 2021;26(3):651.
24. Salah E, Ugochukwu E, Barr AJ, von Delft F, Knapp S, Elkins JM. Crystal structures of ABL-related gene (ABL2) in complex with imatinib, tozasertib (VX-680), and a type I inhibitor of the triazole carbothioamide class. J Med Chem. 2011;54(7):2359-2367.
25. Peruzzotti C, Borrelli S, Ventura M, et al. Probing the binding site of abl tyrosine kinase using in situ click chemistry. ACS Med Chem Lett. 2013;4(2):274-277.
26. Irgit A, Kamıs R, Sever B, et al. Structure and Dynamics of the ABL1 Tyrosine Kinase and Its Important Role in Chronic Myeloid Leukemia. Arch Pharm (Weinheim). 2025;358(5):e70005.
27. Schindler T, Bornmann W, Pellicena P, Miller WT, Clarkson B, Kuriyan J. Structural Mechanism for STI-571 Inhibition of Abelson Tyrosine Kinase. Science. 2000;289(5486):1938-1942.
28. Chen VB, Arendall WB, Headd JJ, Keedy DA, Immormino

RM, Kapral GJ, Murray LW, Richardson JS, Richardson DC. MolProbity: all atom structure validation for macromolecular crystallography. Acta Crystallogr D Biol Crystallogr. 2010;66(1):12-21.
29. Davis IW, Leaver-Fay A, Chen VB, Block JN, Kapral GJ, Wang X, Murray LW, Arendall WB, Snoeyink J, Richardson JS, Richardson DC. MolProbity: all-atom contacts and structure validation for proteins and nucleic acids. Nucleic Acids Res. 2007;35:W375–383.
30. O'Boyle NM, Banck M, James CA, et al. Open Babel: An open chemical toolbox. J Cheminform. 2011;3:33.
31. Eberhardt J, Santos-Martins D, Tillack AF, Forli S. AutoDock Vina 1.2.0: New Docking Methods, Expanded Force Field, and Python Bindings. J Chem Inf Model. 2021;61:3891–3898.
32. Allouche A. Software News and Updates Gabedit — A Graphical User Interface for Computational Chemistry Softwares. J Comput Chem. 2011;32:174–182.
33. Dassault Systèmes BIOVIA. Discovery Studio Modeling Environment, Release 2020. San Diego: Dassault Systèmes; 2020.